

HOT DUST CLOUDS WITH PURE GRAPHITE COMPOSITION AROUND TYPE-I ACTIVE GALACTIC NUCLEI

RIVAY MOR¹ & BENNY TRAKHTENBROT¹

Draft version January 21, 2013

ABSTRACT

We fitted the optical to mid-infrared (MIR) spectral energy distributions (SEDs) of ~ 15000 type-I, $0.75 < z < 2$, active galactic nuclei (AGNs) in an attempt to constrain the properties of the physical component responsible for the rest-frame near-infrared (NIR) emission. We combine optical spectra from the Sloan Digital Sky Survey (SDSS) and MIR photometry from the preliminary data release of the Wide Infrared Survey Explorer (WISE). The sample spans a large range of AGN properties: luminosity, black hole mass, and accretion rate. Our model has two components: a UV-optical continuum source and very hot, pure-graphite dust clouds. We present the luminosity of the hot-dust component and its covering factor, for all sources, and compare it with the intrinsic AGN properties. We find that the hot-dust component is essential to explain the (rest) NIR emission in almost all AGNs in our sample, and that it is consistent with clouds containing pure-graphite grains and located between the dust-free broad line region (BLR) and the “standard” torus. The covering factor of this component has a relatively narrow distribution around a peak value of ~ 0.13 , and it correlates with the AGN bolometric luminosity. We suggest that there is no significant correlation with either black hole mass or normalized accretion rate. The fraction of hot-dust-poor AGNs in our sample is $\sim 15 - 20\%$, consistent with previous studies. We do not find a dependence of this fraction on redshift or source luminosity.

Subject headings: catalogs — galaxies: active — infrared: galaxies

1. INTRODUCTION

The unification scheme of active galactic nuclei (AGNs) requires an anisotropic obscuring structure that surrounds the central accreting black hole (e.g., Krolik & Begelman 1988; Antonucci 1993). In this picture, the bulk of the radiation from the central engine is absorbed by the obscuring structure (commonly referred to as the torus) and re-emitted mainly in mid-infrared (MIR) wavelengths.

A component of very hot dust at the innermost edge of the torus has been suggested in the past (e.g., Neugebauer et al. 1987; Barvainis 1987), and in recent years is increasingly being supported by observations. Reverberation measurements of nearby AGNs suggest that the near infrared (NIR) emission in these sources is dominated by thermal radiation from hot dust very close to the central source (few tens of light days; e.g., Minezaki et al. 2004; Suganuma et al. 2006). Other studies fitted the NIR-MIR spectral energy distributions (SEDs) of AGNs using a blackbody spectrum to represent emission from hot dust in the inner region of the torus (e.g., Kishimoto et al. 2007; Riffel et al. 2009; Mor et al. 2009, hereafter M09; Deo et al. 2011). More recently Landt et al. (2011) found similar results by fitting only the optical-NIR SED of 23 AGNs. The modeled temperature of this component is found to be high, $\gtrsim 1200\text{K}$, regardless of the AGN luminosity and consistent with pure-graphite dust composition (M09). Several studies have shown that the luminosity of the NIR excess emission correlates with that of the central engine (e.g., Gallagher et al. 2007, and references therein) with a slope close to unity. However, it is yet unclear whether this hot-dust component is related to other AGN properties such as its mass (M_{BH}) or normalized accretion rate (L/L_{Edd}).

Although hot dust seems to be a common feature of AGNs, several recent studies have suggested that a certain fraction

of the AGN population lacks such a component. Jiang et al. (2010) found two $z \simeq 6$ QSOs without any detectable emission from hot dust (using *Spitzer* MIR photometry). These were dubbed “hot-dust free” QSOs. Hao et al. (2010) and more recently Hao et al. (2011) found a sizable amount of type-I AGNs with unusually weak NIR emission in several large samples of type-I AGNs. These were dubbed “hot-dust-poor” (HDP; hereafter we adopt this notation) AGNs. These authors found that the fraction of HDP AGNs increases with redshift from 6% at low redshift ($z < 2$) to 20% at higher redshift ($2 < z < 3.5$). We note that all the studies mentioned here are limited to relatively small samples, and use highly simplified emission models.

In this letter we use the recently published preliminary data release of the Wide Infrared Survey Explorer (WISE; Wright et al. 2010), together with the seventh data release of the Sloan Digital Sky Survey (SDSS/DR7; Abazajian et al. 2009) to construct ~ 15000 UV to NIR SEDs of type-I AGNs. We apply spectral decomposition using novel models to deduce the properties of the hot dust, and test these properties against different intrinsic AGN properties.

2. SAMPLE SELECTION AND SPECTRAL DECOMPOSITION

We aim to study a large and uniformly selected sample of type-I AGNs, for which L_{bol} , M_{BH} and L/L_{Edd} can be reliably measured, and the WISE bands (at $\sim 3.4, 4.6$, & $11.6 \mu\text{m}$) cover the rest-frame wavelength range of 1 to $5 \mu\text{m}$, where the emission originating from the hot dust is expected to peak. At longer wavelengths (i.e., those covered by the $\sim 22 \mu\text{m}$ WISE band), the emission from the “standard” torus becomes significant (see Fig. 4 in M09). Thus, we select from the SDSS only high confidence “QSO” sources (i.e. $z_{\text{conf}} > 0.7$) at $0.75 < z < 2$. This query returned 20231 sources within the area covered in the WISE preliminary DR. Cross-matching this sample with the WISE catalog, using a $3''$ search radius, yielded 19116 matched sources. The remaining 1115 sources ($\sim 5.5\%$) probably lie below the flux limit defined for the WISE preliminary DR, of $\sim 0.08\text{mJy}$ in the $3.4 \mu\text{m}$ band.

rivay@wise.tau.ac.il

¹ School of Physics and Astronomy and the Wise Observatory, The Raymond and Beverly Sackler Faculty of Exact Sciences, Tel-Aviv University, Tel-Aviv 69978, Israel

These sources have a similar range of L_{bol} to that of the whole parent sample, and are further discussed in §3. Thus, our analysis of the WISE data provides useful information regarding $\sim 94.5\%$ of optically selected, $0.75 < z < 2$, type-I AGN (see more criteria below).

We further filtered the resultant cross-matched catalog to include only the 17920 sources which have $S/N > 3$ in each of the ~ 3.4 , 4.6 & $11.6 \mu\text{m}$ WISE bands. Our analysis ignores the $\sim 22 \mu\text{m}$ band. The WISE cataloged magnitudes and associated uncertainties were translated to f_{ν} through the published (“iso”) WISE zero points.² The SDSS spectra of all these QSOs were modeled by a comprehensive procedure that is aimed at fitting the broad $\text{Mg II } \lambda 2798$ emission line and the adjacent emission complexes. The procedure is identical to that used in Trakhtenbrot et al. (2011), and similar to other studies (e.g., Shen et al. 2008; Fine et al. 2008). Most importantly, it allows a robust determination of $\text{FWHM}(\text{Mg II})$ and of the monochromatic luminosity at (rest-frame) 3000\AA ($\lambda L_{\lambda}[3000 \text{\AA}]$, hereafter L_{3000}). Further 1571 sources, for which the Mg II fitting procedure failed to provide high-confidence results, were excluded. We also excluded 421 sources with $\log(L_{3000}/\text{erg s}^{-1}) < 45$, which might contain some host-galaxy contribution to their rest-frame NIR SED, and often have SDSS spectra with low S/N. Finally, our sample consists of 15928 QSOs with $45 < \log(L_{3000}/\text{erg s}^{-1}) < 47.25$, which correspond to about 78% of all SDSS selected $0.75 < z < 2$, type-I AGN covered by WISE observations. From these measurements, we deduce M_{BH} using the McLure & Dunlop (2004) prescription. L_{bol} is calculated from L_{3000} by applying a luminosity-dependant bolometric correction, which will be discussed in full detail in a forthcoming publication. Here we only note that these correction factors were independently calibrated using a large sample of $0.5 < z < 0.75$ QSOs, for which L_{bol} could be reliably derived by the Marconi et al. (2004) prescription. The bolometric corrections applied to the SDSS/WISE sample range between about 3, for the most luminous sources, and 4.2, for the faintest. These values are lower, by a factor of $\sim 1.5 - 1.7$, than those of Richards et al. (2006) or Elvis et al. (1994), since they avoid the double-counting of the re-processed IR emission (see the detailed discussion in Marconi et al. 2004). The resultant range in $\log(L_{\text{bol}}/\text{erg s}^{-1})$ is $45.6 - 47.7$. We estimated the accretion rate as $L/L_{\text{Edd}} = L_{\text{bol}}/(1.5 \times 10^{38} M_{\text{BH}})$.

The SDSS/WISE SED of each source in our sample is fitted to constrain the properties of the hot-dust component that dominates the NIR wavelength range. To focus on continuum emission, every SDSS spectrum was sampled at several continuum bands, around the (rest frame) wavelengths: $1450 - 1475$, $2150 - 2200$, $3030 - 3100$, $4150 - 4250$, $5080 - 5120$, $5600 - 5750$, & $6100 - 6250 \text{\AA}$ (e.g., Vanden Berk et al. 2001). Our models include two different components: a source of UV-optical continuum emission (e.g., an accretion disk) and very hot-dust clouds with pure graphite composition.

To model the central-source continuum emission we assume a power-law function, $L_{\nu} \propto \nu^{\alpha}$. This component has two free parameters, the power-law index and the normalization factor. The power-law index, α , is changed in steps of 0.1 between -1.5 to 1. The second component represents a collection of dusty clouds of gas with a pure-graphite grain

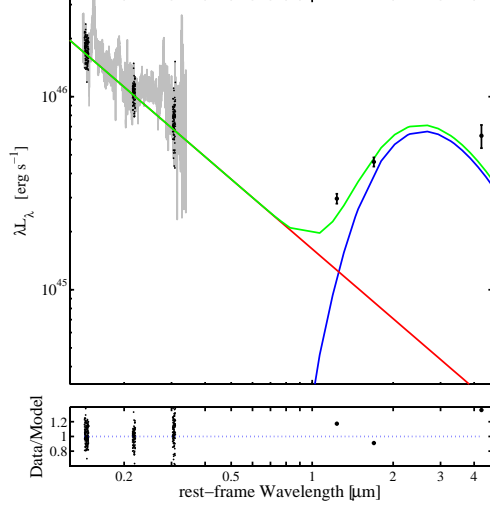


FIG. 1.— Best fit to the SED of SDSS J134154.22+005948.6 ($z = 1.715$) using a combination of power-law (red line) and hot, pure-graphite dust (blue line) components. The original SDSS spectrum is shown in gray and the continuum bands selected for the fitting procedure are highlighted in black. The best fit model is shown in red. The quality of the fit is demonstrated by the ratio between the data and the model (bottom).

composition. The SED of this component is taken from the models of Mor & Netzer (2011), which provide a full discussion of all model assumptions and parameters. In short, this study adopts the “cloud model” of the broad-line region (BLR) and considers the graphite-containing gas to be the extension of the BLR. The model assumes gas composition of $2 Z_{\odot}$, standard ISM-type dust depletion, gas density in the range $\log(n/\text{cm}^{-3}) = 9.3 - 9.8$ and column density in the range $\log(N_{\text{H}}/\text{cm}^{-2}) = 22.3 - 22.7$ at the graphite sublimation radius. While the local emission of the graphite dust depends only on the grain properties, the dust temperature inside the cloud varies by a large factor because of the local grain opacity. Thus a single cloud spectrum appears as a combination of many modified blackbodies. The results of the calculations provide a grid of SEDs that are used in the fitting procedure. For this component there are two free fitting parameters, the distance to the cloud (given a source luminosity) and a normalization factor which determines its luminosity (hereafter L_{HD}). For example, the range of distances for an AGN with $\log(L_{\text{bol}}/\text{erg s}^{-1}) = 46.9$ is 1.3 to 3.5 pc. The fitting procedure uses a standard χ^2 minimization to determine the best fit combination of power-law and hot-dust model. Figure 1 demonstrates the fitting procedure for a representative case. The hot pure-graphite dust component dominates the SED between ~ 2 and $5 \mu\text{m}$. The main caveat of the fitting procedure is the (unknown) contribution to the SED from cooler dust in the torus. As shown in Mor & Netzer (2011), neglecting this component may lead to an overestimation of L_{HD} by merely $\sim 10 - 20\%$. In the following analysis, we do not correct for this systematic uncertainty.

The chosen redshift range, and thus typical AGN luminosities, securely omits any host galaxy dominated SEDs from our sample. To minimize the effect of the (unknown) host-related extinction, we further limit our sample to include only sources for which the best-fit slope of the power-law component satisfies $\alpha > -0.8$. This choice is comparable to those made in other studies of the optical to NIR SED of AGNs. For exam-

² See: http://wise2.ipac.caltech.edu/docs/release/prelim/expsup/figures/sec4_3gt4.gif

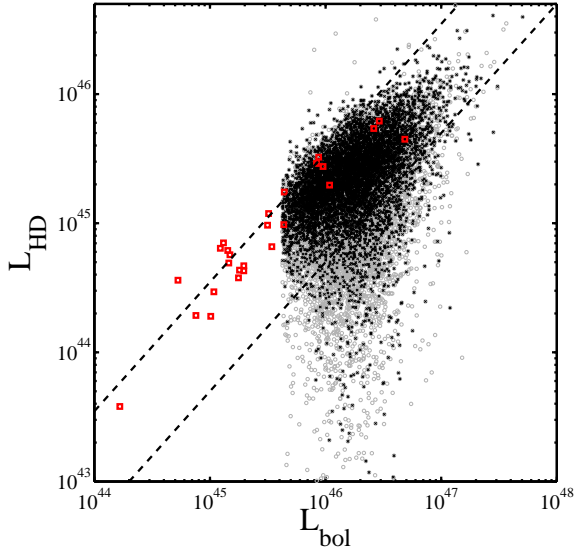


FIG. 2.— Hot-dust luminosity vs. AGN bolometric luminosity. Results from the complete WISE sample studied in this work are shown as gray symbols. Black symbols highlight the sources with $\alpha > -0.4$. The QUEST sample of PG QSOs are shown in red. The dashed lines represent $L_{\text{HD}} \propto L_{\text{bol}}$ (i.e. constant CF_{HD}), with normalization of 0.05 and 0.35.

ple, the Vanden Berk et al. (2001) composite has $\alpha \simeq -0.44$ over the relevant wavelength range, while Hao et al. (2010) show that α ranges between about -0.8 and 0.6, based on the Elvis et al. (1994) SEDs. In any case, omitting this criterion adds only a small fraction of sources and does not significantly change our main results. A more comprehensive analysis of the extinction is beyond the scope of this Letter. The removal of these sources leaves 15077 sources that will be used in the following analysis.

3. RESULTS AND DISCUSSION

The most important parameter of the hot-dust component, determined by the fitting procedure, is L_{HD} . Figure 2 shows a prominent correlation between L_{HD} and L_{bol} . We also highlight a sub-sample of sources with extremely blue continua, which are defined as those with $\alpha > -0.4$, and correspond to the bluest third of the sample (following Gallagher et al. 2007). These sources are presumably less affected by extinction. The distribution of these blue sources in the $L_{\text{HD}} - L_{\text{bol}}$ plane is similar to that of the entire sample, suggesting that host extinction plays only a minor role in our analysis. Results for the QUEST sample (PG QSOs studied in M09; red squares in Fig. 2) were calculated by employing the M09 procedure (using the pure-graphite models) to the ~ 2 to $35 \mu\text{m}$ SEDs.

Assuming that the rest-frame NIR SED is due to reprocessed AGN radiation by the hot-dust clouds, we can deduce the covering factor (CF_{HD}) of the central source by these clouds, defined by $\text{CF}_{\text{HD}} = L_{\text{HD}}/L_{\text{bol}}$ (Maiolino et al. 2007, M09). Fig. 2 clearly indicates that CF_{HD} of the entire population spans a relatively limited range. Indeed, the distribution of CF_{HD} (Figure 3) appears to be fairly concentrated around a peak value of 0.13 (median value is 0.1 with a standard deviation of 0.4 dex). This value is smaller than the one found for the lower luminosity, lower redshift, QUEST sample (~ 0.23). The distribution of CF_{HD} is asymmetric with a clear excess of sources with low CF_{HD} . These sources may represent a different subset of the population with a very small or no hot-dust

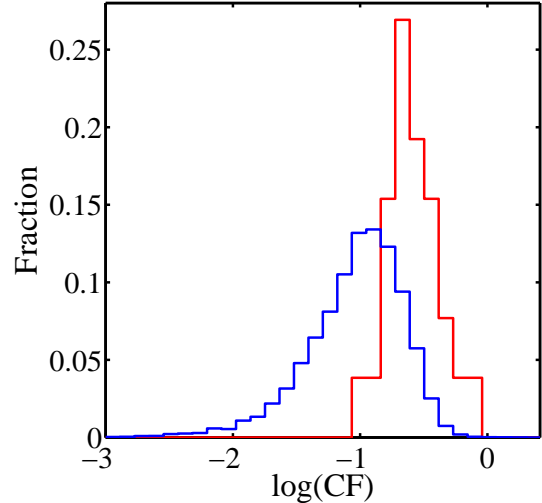


FIG. 3.— Distribution of the hot-dust covering factor. Values of the current study (blue) are generally smaller than those found for the QUEST sample (red) and may be the result of the different luminosity range of the two samples (see Figure 4). The CF_{HD} distribution is asymmetric with a clear excess of low CF_{HD} sources. The peak of the distribution is at ~ 0.13 and the median value is 0.1. Sources with CF_{HD} below a certain luminosity-dependant value may represent the so-called hot-dust-poor or dust-free AGNs.

component. We note that for a small fraction of the sample ($\sim 1.7\%$, 258 sources) the fit does not require a hot-dust component thus resulting in $L_{\text{HD}} = 0$ and $\text{CF}_{\text{HD}} = 0$. We add these sources to the sub-group of HDP AGNs discussed below.

Fig. 4 presents a clear anti-correlation between CF_{HD} and L_{bol} . This trend is further confirmed by both Pearson's and Spearman's rank correlation tests (p value $\ll 0.01$ for both tests). In particular, the typical CF_{HD} decreases from ~ 0.2 for sources with $\log(L_{\text{bol}}/\text{erg s}^{-1}) \simeq 45.6$ to ~ 0.09 for sources with $\log(L_{\text{bol}}/\text{erg s}^{-1}) \simeq 46.6$. We verified that a similar relation is recovered even if one calculates L_{bol} with the commonly used, uniform (and overestimated; see §2) bolometric correction of 5.15 or 5.62 (e.g., Elvis et al. 1994; Richards et al. 2006). Several earlier studies suggested a similar trend (e.g., Wang et al. 2005; Maiolino et al. 2007; Treister et al. 2008), however these were based on the total MIR emission which translates to the covering factor of the entire dusty structure, and not just the hot dust. Gallagher et al. (2007) suggest that this $\text{CF}_{\text{HD}} - L_{\text{bol}}$ anti-correlation may be a manifestation of dust extinction. We therefore verified that this trend persists for the sub-sample of blue sources, defined above. We further checked whether the $\text{CF}_{\text{HD}} - L_{\text{bol}}$ relation is due to the higher abundance of more luminous AGNs towards higher redshifts, using a sub-sample of 3837 sources which reside in a narrow luminosity range (0.2 dex) around $\log(L_{\text{bol}}/\text{erg s}^{-1}) \simeq 46.3$. Although this sub-sample spans almost the entire redshift range of the original sample, no correlation is found between CF_{HD} and redshift.

The physical mechanism responsible for the decrease of covering factor with L_{bol} is still undetermined. One possibility is a “receding torus” scenario (Lawrence 1991), where higher luminosity implies larger dust sublimation distance, and hence an obscuring structure that is located farther away from the center. In this scenario, however, the geometry of the hot-dust clouds must be toroidal and have a constant height. Another possibility is that the $\text{CF}_{\text{HD}} - L_{\text{bol}}$ anti-correlation is analogous to the anti-correlation found between the equivalent width of different BLR lines ($\text{H}\beta$ and C IV) and AGN

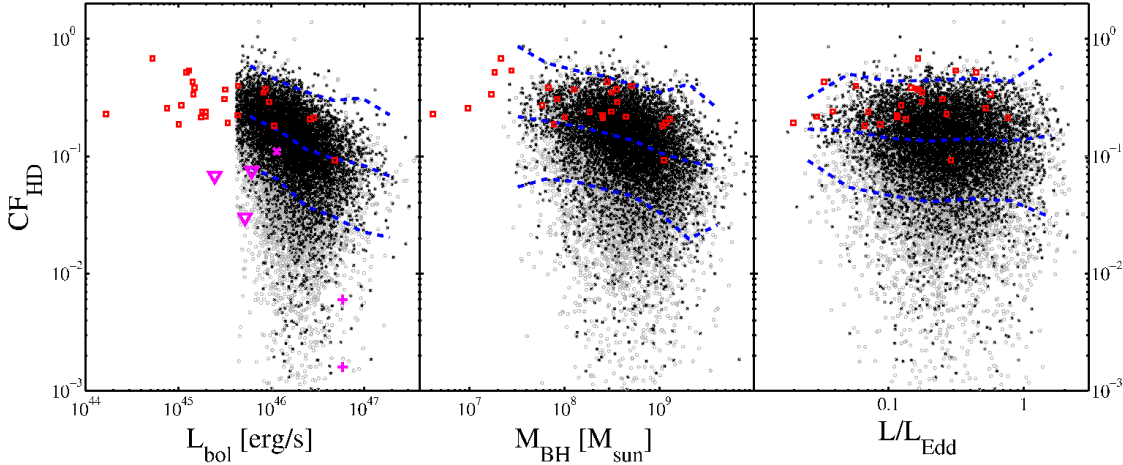


FIG. 4.— Hot-dust covering factor vs. AGN properties. Symbols as in Fig. 2. Left: CF_{HD} decreases with increasing L_{bol} . Magenta markers represent the mean SED of Elvis et al. (1994), scaled to $\log(L_{bol}/\text{erg s}^{-1}) = 46$ (cross); the three examples of hot-dust-poor objects of Hao et al. (2010, triangles) and the two $z \simeq 6$ dust-free QSOs of Jiang et al. (2010, plus signs). The correlations with M_{BH} and L/L_{Edd} (middle and right panels) are much less significant. In all panels, dashed black lines represent the peak of the CF_{HD} distribution and the 3σ -equivalent range - see text

luminosity (e.g., Netzer et al. 2004; Baskin & Laor 2005).

The correlations between CF_{HD} and M_{BH} and L/L_{Edd} (Fig. 4, middle and right panels) are much less significant. We interpret these as the result of the marginal dependence of both M_{BH} and L/L_{Edd} on the source luminosity. This is further confirmed by the fact that these marginal correlations disappear completely in the $\log(L_{bol}/\text{erg s}^{-1}) \simeq 46.3$ sub-sample mentioned above. However, the large scatter makes it difficult to securely determine which correlation is more fundamental. We suggest that the apparent CF_{HD} is sensitive to the immediate irradiating flux from the central source, but does not depend on the evolutionary stage of the accreting super-massive black hole (SMBH).

For a certain fraction of the sources, the hot-dust a component is much less prominent. First, as noted above, $\sim 1.7\%$ of the sources have $L_{HD} = 0$ and thus $CF_{HD} = 0$. These sources spread the entire range of L_{bol} . Second, there is a non negligible population of sources with significantly lower CF_{HD} values than the main locus of sources (Fig. 4). There is no corresponding population of high- CF_{HD} outliers. Fig. 4 illustrates this using the boundaries of the 99th percentiles of the CF_{HD} distribution. The percentiles are calculated by assuming that the CF_{HD} distribution should be symmetrical around the peak and mirroring the high- CF_{HD} side of the distribution. This is done in each (0.2 dex) luminosity bin separately. We suggest that all the points which lie below the lower dashed line in Fig. 4 can be regarded as HDP AGNs. Thus, we are able to provide an HDP criterion which depends on L_{bol} . For example, for $\log(L_{bol}/\text{erg s}^{-1}) = 46$ all sources with $CF_{HD} \lesssim 0.06$ may be considered as HDP AGNs.

The total fraction of HDP AGNs in our sample is $\sim 16.2\%$ (2439 sources out of 15077, including the 258 sources with $CF_{HD} = 0$). This number is in rough agreement with that reported by Hao et al. (2010) and Hao et al. (2011). We do not find a significant dependence of this fraction with either luminosity or redshift. We stress that using a HDP criterion that is independent of AGN luminosity can result in false correlations of the fraction of HDP AGNs with either luminosity or redshift. The latter may be a consequence of selection biases of high luminosity sources towards higher redshifts. As

mentioned in §2, 1115 sources ($\sim 5.5\%$ of the total SDSS detections) probably lie below the flux limit defined for the preliminary DR of WISE. These sources may also represent HDP AGNs, thus should be added to the total fraction mentioned above ($\sim 16.2\%$).

As mentioned in §1, Jiang et al. (2010) suggested that a significant fraction of $z \simeq 6$ AGNs are hot-dust free, i.e. lacking any emission from a hot, dusty component. Moreover, these authors claim that such systems are not observed at lower redshifts. Taken at face value, our $CF_{HD} = 0$ sources can be regarded as the $z < 2$ counterparts of the $z \simeq 6$ hot-dust free AGNs. These are indeed rare at low redshifts. However, the hot-dust free AGNs of Jiang et al. (2010) have only upper limits in the (rest-frame) IR bands, which place them in our HDP AGN regime (see Fig. 4). Thus, our sample might offer many more $z < 2$ sources that correspond to the hot-dust free notion of Jiang et al. (2010), from both the WISE-undetected sub-sample ($\sim 5.5\%$) and the HDP AGN sub-sample ($\sim 16.2\%$). We also note that variability between the SDSS and WISE observational epochs would not effect the estimation of the fraction of HDP AGNs for large samples. It may, however, account for some of the scatter observed in the symmetric part of the CF_{HD} distribution.

We have demonstrated that the rest-frame NIR emission of the vast majority ($\sim 80\%$) of type-I AGNs in our unprecedentedly large sample can be explained by emission from hot, pure-graphite dust clouds. These clouds reside at distances greater by a factor of about 3 – 10 than the BLR clouds, and have a typical CF_{HD} of ~ 0.13 . The lack of a significant correlation between CF_{HD} and M_{BH} stands in contrast to the result of Jiang et al. (2010), who suggested that such a relation only exists at very high redshifts ($z \simeq 6$), where dusty structures around AGNs were not yet fully developed. Interestingly, we do not find any significant correlation between CF_{HD} and either L/L_{Edd} or redshift, despite the fact that our sample effectively covers a wide range in these properties ($0.05 \lesssim L/L_{Edd}$ and $0.75 < z < 2$). We suggest that previous reports of a decrease in CF_{HD} , and an increase in the fraction of HDP AGNs, with increasing redshift, may be due to a combination of the selection of high-luminosity sources at high redshifts

and the $CF_{\text{HD}}-L_{\text{bol}}$ anti-correlation reported here. However, the small overlap in L_{bol} between the low- z QUEST sample and the SDSS/WISE sample, and the limited range of L_{bol} for SDSS/WISE sources, at a chosen redshift, inhibits us from testing this issue further.

To fully understand the *evolution* of hot dusty structures around accreting SMBHs, all these trends should be tested in large samples of high redshift type-I quasars, for which L_{bol} , M_{BH} and L/L_{Edd} were reliably measured (e.g., Netzer et al. 2007; Willott et al. 2010; Trakhtenbrot et al. 2011). As demonstrated in this *Letter*, WISE data provide the optimal way to preform such studies, owing to its wide areal coverage and relatively deep flux limit. In addition, WISE covers the wavelength range where hot-dust emission dominates the SED of AGNs, thus providing more direct probes of this emis-

sion at high-redshift sources than NIR data.

We thank Hagai Netzer for providing the radiative models used in this work and for many helpful comments. Funding for this work has been provided by the Israel Science Foundation grant 364/07 and the DFG via German-Israeli Cooperation grant STE1869/1-1.GE625/15-1. This publication makes use of data products from the Wide-field Infrared Survey Explorer, which is a joint project of the University of California, Los Angeles, and the Jet Propulsion Laboratory/California Institute of Technology, funded by the National Aeronautics and Space Administration. This study makes use of data from the SDSS (see: <http://www.sdss.org/collaboration/credits.html>).

REFERENCES

- Abazajian, K. N., et al. 2009, *The Astrophysical Journal Supplement Series*, 182, 543
- Antonucci, R. 1993, *Annual Review of Astronomy and Astrophysics*, 31, 473
- Barvainis, R. 1987, *The Astrophysical Journal*, 320, 537
- Baskin, A., & Laor, A. 2005, *MNRAS*, 356, 1029
- Deo, R. P., Richards, G. T., Nikutta, R., Elitzur, M., Gallagher, S. C., Ivezić, v., & Hines, D. 2011, *The Astrophysical Journal*, 729, 108
- Elvis, M., et al. 1994, *The Astrophysical Journal Supplement Series*, 95, 1
- Fine, S., et al. 2008, *Monthly Notices of the Royal Astronomical Society*, 390, 1413
- Gallagher, S. C., Richards, G. T., Lacy, M., Hines, D. C., Elitzur, M., & StorrieLombardi, L. J. 2007, *The Astrophysical Journal*, 661, 30
- Hao, H., Elvis, M., Civano, F., & Lawrence, A. 2011, *The Astrophysical Journal*, 733, 108
- Hao, H., et al. 2010, *The Astrophysical Journal*, 724, L59
- Jiang, L., et al. 2010, *Nature*, 464, 380
- Kishimoto, M., Hönig, S. F., Beckert, T., & Weigelt, G. 2007, *Astronomy and Astrophysics*, 476, 713
- Krolik, J. H., & Begelman, M. C. 1988, *The Astrophysical Journal*, 329, 702
- Landt, H., Elvis, M., Ward, M. J., Bentz, M. C., Korista, K. T., & Karovska, M. 2011, *Monthly Notices of the Royal Astronomical Society*, 414, 218
- Lawrence, A. 1991, *Royal Astronomical Society*, 252, 586
- Maiolino, R., Shemmer, O., Imanishi, M., Netzer, H., Oliva, E., Lutz, D., & Sturm, E. 2007, *Astronomy and Astrophysics*, 468, 979
- Marconi, A., Risaliti, G., Gilli, R., Hunt, L. K., Maiolino, R., & Salvati, M. 2004, *Monthly Notices of the Royal Astronomical Society*, 351, 169
- McLure, R. J., & Dunlop, J. S. 2004, *Monthly Notices of the Royal Astronomical Society*, 352, 1390
- Minezaki, T., Yoshii, Y., Kobayashi, Y., Enya, K., Suganuma, M., Tomita, H., Aoki, T., & Peterson, B. A. 2004, *The Astrophysical Journal*, 600, L35
- Mor, R., Netzer, H., & Elitzur, M. 2009, *The Astrophysical Journal*, 705, 298
- Mor, R., & Netzer, H. 2011, Submitted to *Monthly Notices of the Royal Astronomical Society*
- Netzer, H., Shemmer, O., Maiolino, R., Oliva, E., Croom, S., Corbett, E., & di Fabrizio, L. 2004, *ApJ*, 614, 558
- Netzer, H., Lira, P., Trakhtenbrot, B., Shemmer, O., & Cury, I. 2007, *The Astrophysical Journal*, 671, 1256
- Neugebauer, G., Green, R. F., Matthews, K., Schmidt, M., Soifer, B. T., & Bennett, J. 1987, *The Astrophysical Journal Supplement Series*, 63, 615
- Richards, G. T., et al. 2006, *The Astrophysical Journal Supplement Series*, 166, 52
- Riffel, R. A., Storchi-Bergmann, T., Dors, O. L., & Winge, C. 2009, *Monthly Notices of the Royal Astronomical Society*, 393, 783
- Shen, Y., Greene, J. E., Strauss, M. A., Richards, G. T., & Schneider, D. P. 2008, *The Astrophysical Journal*, 680, 169
- Suganuma, M., et al. 2006, *The Astrophysical Journal*, 639, 46
- Trakhtenbrot, B., Netzer, H., Lira, P., & Shemmer, O. 2011, *The Astrophysical Journal*, 730, 7
- Treister, E., Krolik, J. H., & Dullemond, C. 2008, *The Astrophysical Journal*, 679, 140
- Vanden Berk, D. E., et al. 2001, *The Astronomical Journal*, 122, 549
- Wang, J.-M., Zhang, E.-P., & Luo, B. 2005, *The Astrophysical Journal*, 627, L5
- Willott, C. J., et al. 2010, *The Astronomical Journal*, 140, 546
- Wright, E. L., et al. 2010, *The Astronomical Journal*, 140, 1868